Flux limited schemes: Their classification and accuracy based on total variation stability regions

Article *in* Applied Mathematics and Computation · November 2013

DOI: 10.1016/j.amc.2013.08.027

1 author:

Ritesh Dubey
SRM University
11 PUBLICATIONS **35** CITATIONS

FLUX LIMITED SCHEMES: THEIR CLASSIFICATION AND ACCURACY BASED ON TOTAL VARIATION STABILITY REGIONS *

RITESH KUMAR DUBEY†

Abstract. A classification in terms of accuracy of flux limited high resolution schemes in steep gradient region is done which is based on two different total variation (TV) stability regions. The dependence of the TV stability regions on the smoothness parameter is shown. This dependence relation relates and pave a way to define a common unified TV stability region for both class of schemes. New flux limiters, satisfying the unified TV stability region are also proposed which are robust and work efficiently for both backward (left) and forward (right) moving solution profiles. Main significant feature of this classification is that it can improve the accuracy of all existing flux limiters based schemes. Numerical results on linear test problems are given to support the theoretical discussion.

Key words. High resolution schemes; Flux limiters, TVD region; Smoothness parameter; Hyperbolic equations.

AMS subject classifications. 35L65; 65M06; 65M12

1. Introduction. It has been around three decade since CFD community is celebrating the class of high resolution schemes (HRS). The term high resolution scheme coined by Harten represents a class of conservative schemes which crisply resolve discontinuities like contacts, shocks without exhibiting spurious oscillations and give at least second order of accuracy for smooth solutions [3]. Various approaches and methods have been proposed to design such schemes e.g. essentially non-oscillatory (ENO) [17], weighted essential non-oscillatory schemes (WENO) [4] and high resolution total variation diminishing (HRTVD) schemes using flux limiters [19, 6]. A good overview on these methods can be found in [11, 20, 10]. The high resolution total variation diminishing (HRTVD) schemes have been used extensively for excellent numerical results and theoretical support in terms of non-linear stability and entropy satisfaction [24] . In this work, the focus is on the HRTVD schemes using flux limiters.

Among all, the approach proposed by Sweby can be considered as a representative framework for designing Lax-Wendroff type HRTVD schemes using flux limiters [19, 2, 26, 21]. More importantly a total variation (TV) stability region is given for flux limiters to yield total variation diminishing schemes in [19]. Later a variety of high resolution schemes as well as new flux limiters [15, 16, 8, 12, 7] are proposed to improve numerical performance in one

*supported by DST fast track project

†Research Institute, SRM University, Kattankulathur, Tamilnadu 600036 (riteshkd@gmail.com).

way or other. Recently a comparative study of various flux limiters was done for solid gas reaction problems in [5]. In fact a detailed study on desirable properties of these flux limiters to yield high resolution TVD schemes are given in [1, 13, 23]. The most unique feature for all these limiters is that their graph pass within the TVD stability region proposed in [19] either completely or for up to a finite positive value of smoothness parameter. Despite of such tremendous development in the area of TVD schemes, it seems that no attempts were made to find alternate TVD region except in [9, 21]. Using diffusive centered difference first order flux, centered high resolution TVD schemes and flux limiters are proposed in [21]. A TV stability region is given for centered limiters in terms of CFL number which can be reduced to TV stability region given in [19]. In [9], a general framework is proposed for constructing second order upwind high resolution TVD schemes using flux limiters. An entirely new TV stability region and a class of new limiters for proposed schemes are designed which satisfy the proposed TVD region.

As far the classification of such high resolution schemes and flux limiters is concern few attempts are made but mainly (to the best of knowledge of the author) based on central and upwind nature of discretization. These schemes are classified into symmetric schemes based on central discretization in [26] and upwind schemes based on upwind discretization [22, 6, 9] respectively. In [25], flux limiters are also classified as symmetric and upwind type. A qualitative and quantitative comparison is done on some TVD Lax-Wendroff methods using centered and upwind biased flux limiters in [14]. In [21], a classification of HR scheme is done into centered and upwind TVD schemes which is based on choosing centered or upwind diffusive first order accurate numerical flux in the construction.

The flow of the paper goes as follows: As pre-requisite for discussion in section 3, we give a summary on construction of flux limiter based high resolution schemes in section 2. In section 3, we characterize high resolution TVD schemes based on TV stability regions for flux limiters into two classes. An investigation of the relation between the TVD regions and their dependence on the smoothness parameter is done in section 4. An unified universal TV stability region is proposed along with new universal flux limiters in 4.1. Numerical results are given in 5.

2. High resolution TVD schemes using flux limiters . In this section, we give a brief idea on the construction of high resolution schemes using flux limiters for the completeness and clarity on the classification of these schemes. For clarity, we discuss the idea for the

following linear hyperbolic problem though it holds for the non-linear case also.

$$\frac{\partial u}{\partial t} + \frac{\partial f(u)}{\partial x} = 0, f(u) = au, \;\; 0 \neq a \in \mathbf{R}, \;\; (x,t) \in \mathbf{R} \times \mathbf{R}^{+}. \tag{2.1}$$

Here u denotes the convection variable and a is the constant characteristics speed associated with (2.1). Divide the spatial and temporal space into N equal length cells $[x_{i-\frac{1}{2}}, x_{i+\frac{1}{2}}],\ i = 0, 1, \ldots N$ and M intervals $[t^n, t^{n+1}],\ n = 0, 1, \ldots, M$ respectively, where $x_{i\pm\frac{1}{2}}$ is called the cell interface and t^n denotes the n^{th} time level. We know that a conservative numerical approximation for above equation is obtained by

$$\bar{u}_i^{n+1} = \bar{u}_i^n - \lambda \left(\mathcal{F}_{i+\frac{1}{2}} - \mathcal{F}_{i-\frac{1}{2}} \right) \tag{2.2}$$

where $\Delta x = x_{i+\frac{1}{2}} - x_{i-\frac{1}{2}}$, $\Delta t = t^{n+1} - t^n$ and $\lambda = \frac{\Delta t}{\Delta x}$. $\mathcal{F}_{i+\frac{1}{2}}$ is a time-integral average of the flux function at the cell interface and $\bar{u}_i^n$ is the spatial cell-integral average defined as,

$$\bar{u}_i^n \approx \frac{1}{\Delta x} \int_{x_{i-\frac{1}{2}}}^{x_{i+\frac{1}{2}}} u(x, t^n) dx, \;\; \mathcal{F}_{i+\frac{1}{2}} \approx \frac{1}{\Delta t} \int_{t^n}^{t^{n+1}} f(u(x_{i+\frac{1}{2}}, t)) dt. \tag{2.3}$$

The choice of the numerical flux function $\mathcal{F}_{i\pm\frac{1}{2}}$ governs the spatial performance like accuracy, dissipation, numerical oscillations or shock capturing feature of resulting conservative scheme.

DEFINITION 2.1. *A conservative scheme (2.2) is said to be TVD if* $TV(\bar{u}^{n+1}) \leq TV(\bar{u}^n),\ \forall n$, *where total variation of grid function* $\bar{u}$ *at time level* n *is defined as*

$$TV(\bar{u}^n) = \sum_{i=-\infty}^{+\infty} \left| \bar{u}_{i+1}^n - \bar{u}_i^n \right|.$$

The general idea of constructing high resolution scheme is to define its numerical flux $\mathcal{F}^{hrs}_{i+\frac{1}{2}}$ as a combination of a dissipative non-oscillatory low order numerical flux $\mathcal{F}^{l}_{i+\frac{1}{2}}$ and non-dissipative oscillatory high order flux $\mathcal{F}^{h}_{i+\frac{1}{2}}$ using flux limiter function ϕ as follows,

$$\mathcal{F}^{hrs}_{i+\frac{1}{2}}(r_i) = \mathcal{F}^{l}_{i+\frac{1}{2}} + \phi(r_i) \left(\mathcal{F}^{h}_{i+\frac{1}{2}} - \mathcal{F}^{l}_{i+\frac{1}{2}} \right). \tag{2.4}$$

In general limiter ϕ is taken as function of smoothness parameter r which measures the smoothness of the solution profile. r is defined as function of ratio of consecutive gradients of the solution of (2.1).

The flux limiter ϕ is defined in such a way that it diminish to zero in the solution region with extreme points or discontinuities, hence scheme results into first order dissipative approximation for such solution region. Limiter ϕ takes a value close to one to give high accurate approximation for smooth region of solution.

3. TV stability regions: Classification. For the sake of discussion, here we take combination of numerical flux function of first order upwind and three representative second order accurate schemes viz Lax-Wendroff, second order upwind and Beam-Warming schemes respectively to construct flux limited schemes for linear problem (2.1). The numerical flux function of Lax-Wendroff flux limited high resolution scheme can be constructed as in [19]

$$\mathcal{F}^{LxWflm}_{i+\frac{1}{2}}(r_i) = a\bar{u}_i + \frac{1}{2}a(1-a\lambda)\phi(r_i)\left(\bar{u}_{i+1} - \bar{u}_i\right),\ a > 0, \tag{3.1}$$

Numerical flux function of second order upwind flux limited method in [6] can be written as

$$\mathcal{F}^{IIupflm}_{i+\frac{1}{2}}(r_i) = a\bar{u}_i + \frac{1}{2}a\lambda\psi(r_i)\left(\bar{u}_i - \bar{u}_{i-1}\right),\ a > 0. \tag{3.2}$$

Similar to second order upwind flux limited method one can obtain Beam-Warming flux limited method

$$\mathcal{F}^{BWflm}_{i+\frac{1}{2}}(r_i) = a\bar{u}_i + \frac{1}{2}a(1-a\lambda)\psi(r_i)\left(\bar{u}_i - \bar{u}_{i-1}\right),\ a > 0. \tag{3.3}$$

where ϕ, ψ are flux limiters and r_i is the smoothness parameter which measure the smoothness of solution and defined as function of consecutive gradients. On Uniform grid it is,

$$r_i = \frac{\bar{u}_i - \bar{u}_{i-1}}{\bar{u}_{i+1} - \bar{u}_i}. \tag{3.4}$$

In order to ensure the TV stability of resulting HR schemes following conditions are given on the flux limiters ϕ and ψ in [19] and [6] respectively using the following results by Harten [3].

LEMMA 3.1. *Consider a conservative scheme in the Incremental form (I-form)*

$$\bar{u}_i^{n+1} = \bar{u}_i^n + \alpha_{i+\frac{1}{2}}\Delta_+\bar{u}_i^n - \beta_{i-\frac{1}{2}}\Delta_-\bar{u}_i^n. \tag{3.5}$$

A sufficient condition for the scheme (3.5) to be TVD is

$$\alpha_{i+\frac{1}{2}} \geq 0,\ \beta_{i-\frac{1}{2}} \geq 0,\ 0 \leq \alpha_{i+\frac{1}{2}} + \beta_{i-\frac{1}{2}} \leq 1. \tag{3.6}$$

THEOREM 3.2. *The resulting conservative scheme using numerical flux function* $\mathcal{F}^{LxWflm}_{i+\frac{1}{2}}(r_i)$ *is TV stable under the CFL condition* $0 \leq a\lambda \leq 1,\ a \geq 0$ *if the flux limiter* $\phi(r)$ *satisfy,*

$$0 \ \leq \frac{\phi(r)}{r} \leq \ 2 \ \textit{and} \ 0 \ \leq \phi(r) \ \leq 2. \tag{3.7}$$

THEOREM 3.3. *The resulting conservative scheme using numerical flux function* $\mathcal{F}_{i+\frac{1}{2}}^{IIupflm}(r_i)$ *is TV stable under the CFL condition* $0 \leq a\lambda \leq \frac{1}{2},\ a \geq 0$ *if the flux limiter* $\psi(r)$ *satisfy,*

$$0 \ \leq r\psi(r) \leq \ 2 \ \textit{and} \ 0 \ \leq \psi(r) \ \leq 2. \tag{3.8}$$

In next result, we give conditions on flux limiter function for flux limited schemes of Beam-Warming type which are same as in Theorem 3.3.

THEOREM 3.4. *The resulting conservative scheme using numerical flux function* $\mathcal{F}_{i+\frac{1}{2}}^{BWflm}(r_i)$ *is TV stable under the CFL condition* $0 \leq a\lambda \leq 1,\ a \geq 0$ *if the flux limiter* $\psi(r)$ *satisfy,*

$$0 \ \leq r\psi(r) \leq \ 2 \ \textit{and} \ 0 \ \leq \psi(r) \ \leq 2. \tag{3.9}$$

Proof. The resulting Beam Warming flux limited scheme while written in conservative I-form (3.5) has,

$$\alpha_{i+\frac{1}{2}} = 0, \beta_{i-\frac{1}{2}} = \left(a\lambda + \frac{a\lambda}{2}(1 - a\lambda)\left(\psi(r_i) - r_{i-1}\psi(r_{i-1})\right)\right)$$

Using Lemma 3.1, for scheme to be TVD, sufficient condition is

$$0 \leq a\lambda + \frac{a\lambda}{2}(1 - a\lambda)\left(\psi(r_i) - r_{i-1}\psi(r_{i-1})\right) \leq 1. \tag{3.10}$$

which can be written as

$$\frac{-2}{1 - a\lambda} \leq \psi(r_i) - r_{i-1}\psi(r_{i-1}) \leq \frac{2}{a\lambda} \tag{3.11}$$

Note under CFL condition $0 \leq a\lambda \leq 1$, $\max \dfrac{-2}{1 - a\lambda} = -2$ and $\min \dfrac{2}{a\lambda} = 2$. Inequality (3.11) holds if,

$$-2 \leq \psi(r_i) - r_{i-1}\psi(r_{i-1}) \leq 2. \tag{3.12}$$

Compound Inequality (3.12) satisfies (after dropping out index i) if

$$0 \ \leq r\psi(r) \leq \ 2 \ \text{and} \ 0 \ \leq \psi(r) \ \leq 2. \tag{3.13}$$

□

The distinct TV stability region for the flux limiter ϕ and ψ can be rewritten as,

$$\mathcal{R}_1 = \{(r, \phi) \in R \times R : 0 \ \leq \phi(r) \leq \ 2\max(r, 0) \ \text{ and } \ 0 \ \leq \phi(r) \ \leq 2\}. \tag{3.14}$$

$$\mathcal{R}_2 : \left\{(r, \psi) \in R \times R : 0 \ \leq \psi(r) \leq \ \frac{2}{\max(r, 0)} \ \text{ and } \ 0 \ \leq \psi(r) \ \leq 2\right\}. \tag{3.15}$$

In [21], a Courant number dependent TVD stability region for proposed centered schemes is derived which reduce to CFL number independent TVD region $\mathcal{R}_1$ in (3.14). Hence one can consider region $\mathcal{R}_1$ as a generic TV stability region for most centered Lax-Wendroff type HRTVD schemes. Similarly region $\mathcal{R}_2$ in (3.15) can be considered generic TV stability region for most upwind Beam-Warming type HRTVD schemes. In the following subsection we discuss both the stability region and formulation.

Note that for the same measure of smoothness parameter r, TV stability regions in (3.14) and (3.15) are different as shown in Figure 3.1. Let the class of high resolution total variation stable schemes with $\mathcal{R}_1$ and $\mathcal{R}_2$ stability region be denoted by $\mathcal{C}^{\mathcal{R}_1}$ and $\mathcal{C}^{\mathcal{R}_2}$ respectively. This classification make sense and quantifies the schemes in terms of order of accuracy. Schemes of one class approximates the steep gradient solution region in opposite way compared to the schemes of other class. Note that in rapidly monotone increasing solution region i.e. $1 >> r \to 0^+$, limiters for $\mathcal{C}^{\mathcal{R}_1}$ schemes must tend to 0 and give first order approximation whereas limiters for $\mathcal{C}^{\mathcal{R}_2}$ schemes can give at least second order accurate approximation. On the other hand in rapidly monotone decreasing solution region i.e. $1 << r \to +\infty$, limiters for $\mathcal{C}^{\mathcal{R}_2}$ class tend to 0 and result into first order approximation whilst limiters for $\mathcal{C}^{\mathcal{R}_1}$ can give higher accuracy (See Figure 5.1 for numerical illustration). A class of flux limiters ($\delta-$limiters, say) which ensure second order of accuracy in smooth region and satisfy TV stable region $\mathcal{R}_2$ is also given in [6] as follows,

$$\psi^{\delta}(r) = \begin{cases} 0, & r \leq 0, \\ \min\left[2, \frac{2}{r}, \frac{1+\delta}{\delta+r}\right], & r > 0, \quad \text{for any fixed } \delta \in [0, \infty). \end{cases} \tag{3.16}$$

Also analogous to classical Minmod limiter i.e,

$$\phi_b^{mm}(r) = max\left(min\left(1,\, br\right), 0\right),\ 1 \leq b \leq 2 \tag{3.17}$$

one can define a diffusive limiter say, $RKminmod$, which satisfy (3.15),

$$\psi_b^{mm}(r) = max\left(min\left(1,\, \frac{b}{r}\right), 0\right),\ 1 \leq b \leq 2 \tag{3.18}$$

Geometrically TV stability region (3.14) along with some of the flux limiters is drawn in Figure 3.1(a). The region (3.15) with limiters (3.16) for $\delta = 1, 9$ and limiter (3.18) is shown in Figure 3.1 (b).

4. TV stable region: Dependence on smoothness parameter. The smoothness parameter r taken in the formulation of flux functions (3.1), (3.2) (or (3.3)) is defined as in (3.4)

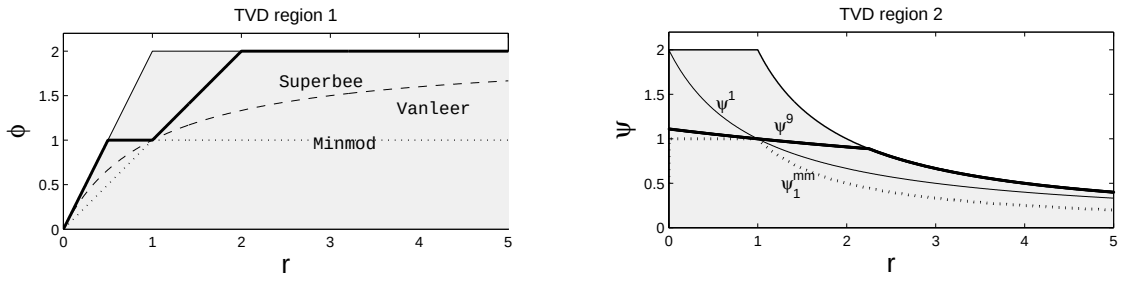

(a) (b)

FIG. 3.1. *TVD regions and some limiter passing through them: $\mathcal{R}_1$ (left) and $\mathcal{R}_2$ (right)*

and despite of same r these schemes have different TV stability region. In fact one can also take the measure of smoothness as $s_i = \dfrac{1}{r_i}$ i.e.,

$$s_i = \frac{\bar{u}_{i+1} - \bar{u}_i}{\bar{u}_i - \bar{u}_{i-1}}. \tag{4.1}$$

This smoothness measure s is indeed taken in literature but to preserve TV stability region $\mathcal{R}_1$ ($\mathcal{R}_2$) for $\mathcal{C}^{\mathcal{R}_1}$ ($\mathcal{C}^{\mathcal{R}_2}$) schemes for (2.1) with negative characteristic speed. In the following, TV stability region for resulting HR schemes is investigated while s is used instead of r as measure of smoothness in (3.1) and (3.2) even though characteristic speed a is positive.

THEOREM 4.1. *The resulting conservative scheme using numerical flux function $\mathcal{F}^{LxWflm}_{i+\frac{1}{2}}(s_i)$ is TV stable under the CFL condition $0 \leq a\lambda \leq 1,\ a > 0$, if the flux limiter $\phi(s)$ satisfy,*

$$0 \ \leq s\phi(s) \leq \ 2 \ \textit{and} \ 0 \ \leq \phi(s) \ \leq 2. \tag{4.2}$$

Proof. The resulting Lax-Wendroff flux limited scheme if written in conservative I-form (3.5) has,

$$\alpha_{i+\frac{1}{2}} = 0 \text{ and } \beta_{i-\frac{1}{2}} = \left(\lambda\, a - \frac{\lambda\, a}{2}(1 - \lambda\, a)\,(\phi(s_{i-1}) - s_i\phi(s_i))\right).$$

Using Lemma 3.1, a sufficient condition for the scheme to be TVD is,

$$0 \leq \left(\lambda\, a - \frac{\lambda\, a}{2}(1 - \lambda\, a)\,(\phi(s_{i-1}) - s_i\phi(s_i))\right) \leq 1 \tag{4.3}$$

Under the linear stability condition $0 \leq \lambda a \leq 1$, inequalities (4.3) satisfy if,

$$-2 \leq -\phi(s_{i-1}) + s_i\phi(s_i) \leq 2,\ \forall i.$$

which satisfies (after dropping out index i) if,

$$0 \leq s\phi(s) \leq 2 \text{ and } 0 \leq \phi(s) \leq 2.$$

which completes the proof. □

Similarly following theorem can be proved

THEOREM 4.2. *The resulting conservative scheme using numerical flux function* $\mathcal{F}^{IIupflm}_{i+\frac{1}{2}}(s_i)$ *is TV stable under the CFL condition* $0 \leq a\lambda \leq \frac{1}{2},\ a > 0$*, if the flux limiter* $\psi(s)$ *satisfy,*

$$0 \leq \frac{\psi(s)}{s} \leq 2 \text{ and } 0 \leq \psi(s) \leq 2. \tag{4.4}$$

In case of negative characteristic speed i.e., $a \leq 0$ in (2.1) we have following analogous results to ensure the TV stability of schemes.

COROLLARY 4.3. *The resulting conservative scheme using numerical flux function* $\mathcal{F}^{LxWflm}_{i+\frac{1}{2}}(r_{i+1})$ *is TV stable under the CFL condition* $-1 \leq a\lambda \leq 0$, $a < 0$, *if the flux limiter* $\phi(r)$ *satisfy,*

$$0 \leq r\phi(r) \leq 2 \text{ and } 0 \leq \phi(r) \leq 2. \tag{4.5}$$

COROLLARY 4.4. *The resulting conservative scheme using numerical flux function* $\mathcal{F}^{LxWflm}_{i+\frac{1}{2}}(s_{i+1})$ *is TV stable under the CFL condition* $-1 \leq a\lambda \leq 0$, $a < 0$, *if the flux limiter* $\phi(s)$ *satisfy,*

$$0 \leq \frac{\phi(s)}{s} \leq 2 \text{ and } 0 \leq \phi(s) \leq 2. \tag{4.6}$$

COROLLARY 4.5. *The resulting conservative scheme using numerical flux function* $\mathcal{F}^{IIupflm}_{i+\frac{1}{2}}(r_{i+1})$ *is TV stable under the CFL condition* $-\frac{1}{2} \leq a\lambda \leq 0,\ a < 0$ *if the flux limiter* $\psi(r)$ *satisfy,*

$$0 \leq \frac{\psi(r)}{r} \leq 2 \text{ and } 0 \leq \psi(r) \leq 2. \tag{4.7}$$

COROLLARY 4.6. *The resulting conservative scheme using numerical flux function* $\mathcal{F}^{IIupflm}_{i+\frac{1}{2}}(s_{i+1})$ *is TV stable under the CFL condition* $-\frac{1}{2} \leq a\lambda \leq 0,\ a < 0$ *if the flux limiter* $\psi(r)$ *satisfy,*

$$0 \leq s\psi(s) \leq 2 \text{ and } 0 \leq \psi(s) \leq 2. \tag{4.8}$$

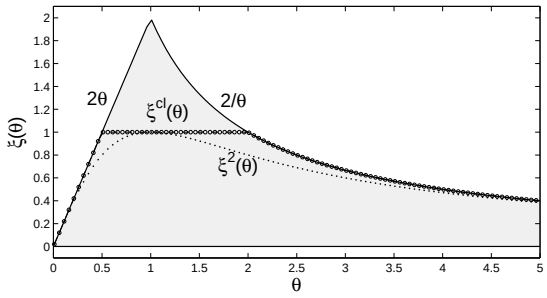

FIG. 4.1. *Unified TVD region along with flux limiters*

REMARK 4.7. All the above conditions on flux limiter functions for second order upwind flux limited method hold true for flux limiter functions for Beam-Warming flux limited method under the CFL condition $|a\lambda| \leq 1$.

REMARK 4.8. Based on above theorems and analogous corollaries, dependence of TV stability region for flux limiter on the measure of smoothness parameter is evident. It can be observed that if a fix measure of smoothness i.e, r (or s) is taken for convection equation irrespective of sign of characteristics speed then HR schemes which belong to class $\mathcal{C}^{\mathcal{R}_1}$ (or $\mathcal{C}^{\mathcal{R}_2}$) for positive characteristic speed will fall into class $\mathcal{C}^{\mathcal{R}_2}$(or $\mathcal{C}^{\mathcal{R}_1}$) respectively for negative characteristic speed.

REMARK 4.9. One can improve accuracy of all existing flux limiters based schemes in steep gradient region by constructing hybrid schemes by judiciously choosing scheme of one class over schemes of other class depending upon measure of smoothness see Figure 5.1(c).

4.1. Unified TV stability region. It can be easily observed that all the flux limiters developed so far for TV stability region $\mathcal{R}_1$ to yield TV stable $\mathcal{C}^{\mathcal{R}_1}$ schemes fail to preserve TV stability when applied on the schemes of class $\mathcal{C}^{\mathcal{R}_2}$. Similarly limiters (3.16) and (3.18) developed for TV region $\mathcal{R}_2$ to yield TV stable $\mathcal{C}^{\mathcal{R}_2}$ schemes fail to give TV stability for schemes of class $\mathcal{C}^{\mathcal{R}_1}$. A unified TV stable region can be deduce for both class of HR schemes as follows,

$$\mathcal{R}_c = \left\{ (\theta, \xi) \in R \times R : 0 \ \leq \theta\, \xi(\theta) \leq \ 2 \ \text{ and } \ 0 \ \leq \frac{\xi(\theta)}{\theta} \ \leq 2 \right\}, \tag{4.9}$$

where $\theta = r$ (or s) and $\xi = \phi$ (or ψ). respectively Note that, the above unified common TV stability region R_c shown in Figure 4.1 can be used to design flux limiters which satisfy this common TV stable region and guarantee second order of accuracy for smooth solution

profile i.e near $r \approx 1$. We propose flux limiters as follows,

$$\xi(\theta) = \xi^n(\theta) = \frac{\theta + |\theta|}{\theta^n + 1},\ n \geq 2,\ \lim_{\theta \to +\infty} \xi \to 0. \tag{4.10}$$

Note that for $n = 1$, we obtain Vanleer flux limiter while for $\theta > 0,\ n = 2$ we obtain van-Albada2 type limiter ($\xi^2(\theta)$) [7]. A more compressive limiter ($\xi^{cl}(\theta)$) can be defined as

$$\xi(\theta) = \xi^{cl}(\theta) = max\left[min\left\{2\theta,\ \frac{2}{\theta},\ 1\right\},\ 0\right]. \tag{4.11}$$

In Figure 4.1 flux limiter (4.10) for $n = 2$ and limiter (4.11) are also shown.

REMARK 4.10. *It can be easily observed that the proposed unified stability region R_c is invariant under any transformation i.e. with respect to change in definition of measure of smoothness or change in the sign of characteristic speed, hence can be considered as universal TV stability region for high resolution total variation diminishing schemes using flux limiters.*

5. Numerical results. The aim of numerical results in this section is to show the difference in the behavior of flux limited schemes on discontinuities or in steep gradient region of solution to support the classification discussed in section 3. Numerical results are presented to show robustness of universal limiters. Numerical results obtained by a hybrid scheme are also given to justify remark 4.9. In all the presented Figures following name convention is used: Results by centered TVD high resolution scheme proposed in [21] for three choice of $\mathcal{F}^l$ as centered first order monotone flux viz: Lax-Friedrichs, FORCE and Godunov [18] are shown by c-lxf, c-force and c-god respectively. Results obtained by flux limited method (3.1), (3.2) and (3.3) and a hybrid scheme are shown by LxWflm, IIupflm, BWflm and hybrid respectively.

5.1. Test for behavior and accuracy. In this section flux limited method of both class are considered alongwith Minmod type limiters to show their performance in steep gradient or discontinuous region. Numerical test are also done by a simple **hybrid** scheme obtained by average of Lax-Wendroff and Beam-Warming flux limited method. Parameter $b = 2$ is taken in these limiters as it ensures second order accuracy for maximum range of $r \geq 0$.

5.1.1. Transport equation. Consider linear transport equation

$$\frac{\partial u}{\partial t} + a\frac{\partial u}{\partial x} = 0, \tag{5.1}$$

where a is characteristic speed. We take $a = 1$ and following initial conditions

$$u(x,0) = \begin{cases} 1, & \text{if } |x| \leq \frac{1}{3}, \\ 0, & else. \end{cases} \tag{5.2}$$

$$u(x,0) = \sin(\pi\, x). \tag{5.3}$$

The exact solution corresponding to initial condition (5.2) has two propagating contact discontinuities. This test is especially taken to depict the accuracy of both class of schemes on capturing the left and right discontinuities in the solution profile. Numerical results obtained with LxWflm and BWflm using Minmod type limiters (3.17) and (3.18) respectively are shown in Figure 5.1(a) and 5.1(b) respectively. Result obtained by average of Lax-Wendroff and Beam-Warming flux limited method (hybrid) using minmod type limiters are shown in 5.1(c).

It can be easily observe from Figure 5.1(a) and 5.1(b) that scheme LxWflm of class $\mathcal{C}^{\mathcal{R}_1}$ give diffusive low order approximation for top of left jump and bottom of right jump whilst bottom of left jump and top of right jump is approximated with higher accuracy. On the other hand scheme BWflm of class $\mathcal{C}^{\mathcal{R}_2}$ show opposite behavior on left and right jumps which supports the discussion in section 3.

It can be easily seen from Figure 5.1(c) that hybrid flux limited scheme is more accurate and captures both discontinuity symmetrically with best resolution by both class of scheme.

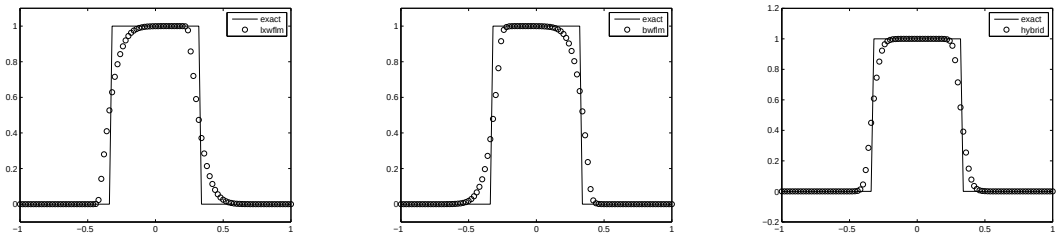

(a) (b) (c)

FIG. 5.1. *Transport equation: Numerical result using minmod limiters $\phi_2^{mm}(r)$ and $\psi_2^{mm}(r)$ respectively with a $\lambda = 0.8$, $N = 50$, $T = 10.0$.*

The periodic initial condition (5.3) with period $T = 2$, has smooth solution region and extreme points at $x = \pm 0.5$. The exact solution convect with out loosing its initial shape and hight. In Table 5.1, L^1 and Ł$^\infty$ error rates are shown exactly after fifteen time period i.e., at $T = 30$ by using Minmod limiter ϕ_2^{mm} and ψ_2^{mm} with LxWflm and BWflm scheme

respectively while for hybrid scheme error rate is also shown corresponding to compressive limiter ξ^{cl}. From numerical results it reflects that the hybrid scheme show better convergence rate for both Minmod and compressive limiters. This improvement is more evident in L^1 error rate.

Minmod Limiter							ξ^{cl} Limiter	
N	LxWflm $\phi_2^{mm}(r)$		BWflm $\psi_2^{mm}(r)$		Hybrid		Hybrid	
	Ł^1	L^∞	Ł^1	L^∞	Ł^1	L^∞	Ł^1	L^∞
10	—	—	—	—	—	—	—	—
20	1.61	2.38	1.81	2.42	2.04	2.58	1.96	2.52
40	1.21	2.31	1.17	2.30	1.61	2.40	1.61	2.36
80	1.60	1.92	1.75	2.12	1.93	2.51	1.94	2.50
160	1.80	2.11	1.87	2.31	2.03	2.39	2.09	2.42
	1.90	2.27	1.92	2.24	2.06	2.31	2.08	2.39

TABLE 5.1

Order of convergence with the mesh refinement for $C = 0.9$ at time $T = 30$.

5.1.2. Burgers equation. Consider following 1D scalar nonlinear Burgers equation

$$\frac{\partial u}{\partial t} + \frac{\partial}{\partial x}\left(\frac{u^2}{2}\right) = 0, \tag{5.4}$$

we consider (5.4) with constant boundary condition and following initial condition

$$u(x,0) = \begin{cases} 0, & \text{if } x \le -\frac{1}{2}, \\ 1, & \text{if } -1 \le x \le 0 \\ 1 - \frac{2x}{3}, & \text{if } 0 \le x \le 3/2 \\ 0 & \text{else .} \end{cases} \tag{5.5}$$

In this test case, due to non-linearity the initial discontinuity at $x = -1/2$ create an rarefaction fan and the initial monotonic solution region in the interval $0 \le x \le 3/2$ evantually results into a moving shock. In this test case it is significantly visible in the numerical results shown in Figure 5.2 that the left rearefaction where the solution is increasing LxWflm show little diffusion and does not resolve foot and head as crisply as BWflm scheme. On the other hand in monotonically decreasing solution region LxWflm perform better then BWflm especially when approximating upper right corner. In this test too, the hybrid scheme give better approximation for both monotonic solution region.

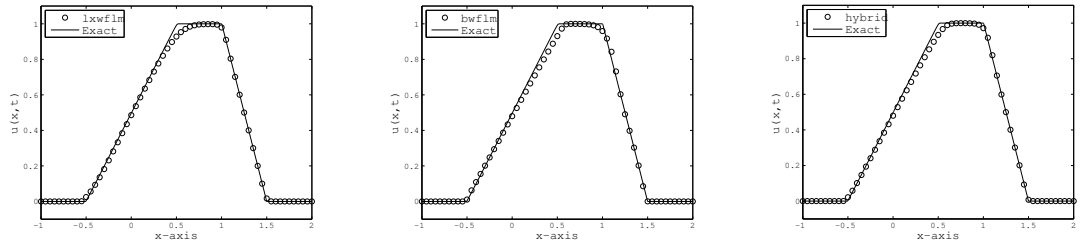

(a) (b) (c)

FIG. 5.2. *Burgers equation: Numerical result using minmod limiters $\phi_2^{mm}(r)$ and $\psi_2^{mm}(r)$ respectively with $\lambda \max_u |f^{'}(u)| = 0.2$, $N = 60$, $T = 1.0$.*

5.2. Results obtained by universal limiters.

5.2.1. Smooth solution case: Separating peaks. In this test case we consider (5.1) with the discontinous advection coefficient given by $a = \begin{cases} -1, & x < 0, \\ 1, & x \geq 0. \end{cases}$ Due to discontinous nature of characteristic speed this test mimic advection in a heterogeneous medium. We consider the following smooth initial condition with steep profile,

$$u(x,\,0) = \begin{cases} |sin(10\pi\, x)|, & 0.1 \leq |x| \leq 0.2, \\ 0, & else. \end{cases} \tag{5.6}$$

Note that the initial solution has two upward peaks which convect in opposite direction and separate due to positive and negative characteristic speed $a = \pm 1$ on right and left side of the point $x = 0$. For the computation of results given in Figure 5.3 and Figure 5.4, same measure of smoothness i.e., $r = \dfrac{\Delta_- \bar{u}_i}{\Delta_+ \bar{u}_i}$ for positive as well negative characteristic speed is used. In Figure 5.3, numerical results obtained by centered and upwind flux limited methods are given for CFL number $a\lambda = 0.45$ at time $T = 1.0$. Note that up to time $T = 1.0$ non-zero initial profile does not touch the computational boundary which make it well-posed. In the computation compressive limiter ξ^{cl} is used. Note that since centered first order flux FORCE is diffusive compared to the GODUNOV and first order upwind flux hence the numerical results c-force is more dissipative compared to the results of upwind TVD schemes in Figure 5.3(b). Note that the high order Lax-Wendroff numerical flux is taken for all these schemes except in IIupflm which takes second order upwind flux.

Figure 5.4(a) and 5.4(b) show the results obtained by scheme $IIupflm$ and $LxWflm$ using $Rkminmod$ ($\psi_1^{mm}(r)$) in (3.18) and classical minmod ($\phi_1^{mm}(r)$) limiter in (3.17) respectively while the smoothness parameter is r defined as in (3.4). Solution is computed

for $T = 1.0,\ CFL = 0.25,\ N = 400$. It can be seen that both the schemes captures the right moving peak with a TVD approximation whereas give oscillatory approximation for left moving peak. These results show that the flux limiter designed for TVD region (3.14) or (3.15) fails for schemes of class $\mathcal{C}^{\mathcal{R}_1}$ or $\mathcal{C}^{\mathcal{R}_2}$ for a fixed definition of measure of smoothness for both direction of characteristic speed.

In order to compare the unified limiters with minmod limiters ($\psi_1^{mm}(\theta)$ and $\phi_1^{mm}(\theta)$) with respective schemes, the measure of smoothness is taken depending on direction of flow i.e.,

$$\theta = \begin{cases} r, & \text{if } a \geq 0, \\ s, & \text{if } a < 0, \end{cases} \tag{5.7}$$

where r and s are defined as (3.4) and (4.1) respectively. In Figure 5.5, we give zoom view of the numerical results obtained by upwind high resolution schemes [6] and [19]. These results show that the limiter $\xi^2(\theta)$ give comparable results with minmod type limiters whilst $\xi^{cl}(\theta)$ give less dissipation and better approximation for the solution.

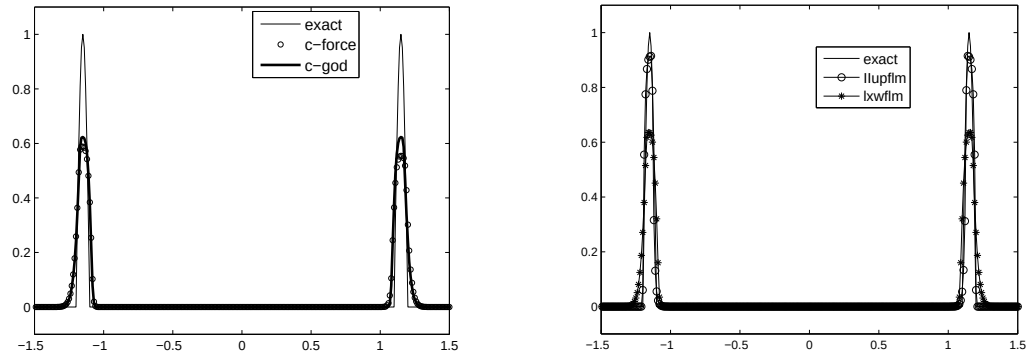

(a) (b)

FIG. 5.3. *Numerical result of centered and upwind high resolution scheme using compressive limiter* ($\xi^{cl}(r)$) *with a* $\lambda = 0.45, T = 1.0,\ N = 400$.

5.2.2. Linear convection: Contact Discontinuity case. In order to show the performance of proposed limiter (ξ^{cl}) for discontinuous solution profile, we consider the equation (5.1) with $a = 1.0$ and the following discontinuous initial condition,

$$u(x,0) = \begin{cases} 1, & \text{if } \ 0.1 \leq x \leq 0.4, \\ 0, & \text{else.} \end{cases} \tag{5.8}$$

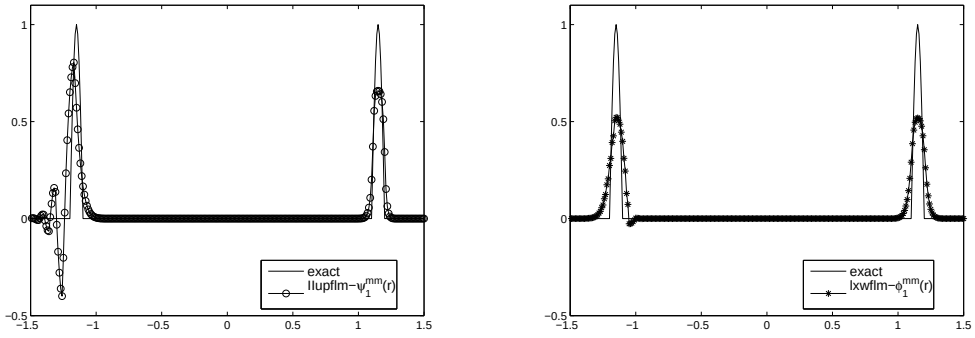

(a) (b)

FIG. 5.4. *Numerical result of upwind high resolution scheme using minmod type limiter for data* $a\,\lambda = 0.25, T = 1.0,\ N = 400$

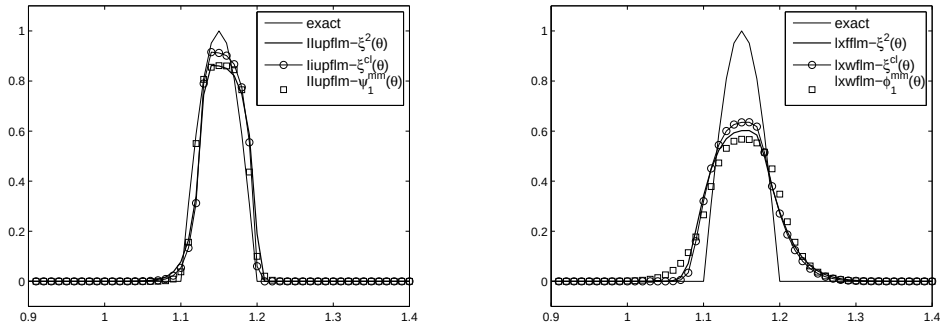

(a) (b)

FIG. 5.5. *Solution by upwind high resolution schemes IIupflm and LxWflm using limiter* $\xi^2(\theta)$ *in (4.10) for* $n = 2$*, limiter* $\xi^{cl}(\theta)$ *in (4.11) and minmod type limiters.*

In Figure 5.6(a), zoom in solution obtained by some high resolution schemes using compressive limiter ϕ^{cl} in (4.11) at time $T = 2.0$ is given. The computational domain in space $[0, 3]$ is divided into $N = 90$ intervals for $CFL = 0.8$. Result shows that even for limiter ξ^{cl} scheme LxWflm of class $\mathcal{C}^{\mathcal{R}_1}$ capture the foot of the left discontinuity much crisply compared BWflm of class $\mathcal{C}^{\mathcal{R}_2}$ but for foot of right discontinuity is captured in opposite way.

In order to show that the universal limiters are independent of the choice the measure of smoothness for both class of schemes. In Figure 5.6(b), we show the result obtained by using universal limiters $\xi^2(\theta)$ in HR schemes IIupflm-r (LxWflm-r) and IIupflm-s (LxWflm-s) for both choice of smoothness parameter $\theta = r$ and $\theta = s$ respectively. Note that the change

in choice of measure r or s interchange the TV stability region for one class (e.g., $\mathcal{C}^{\mathcal{R}_1}$) to another class (e.g., $\mathcal{C}^{\mathcal{R}_2}$).

REMARK 5.1. Using these universal limiters $\xi^2(\theta)$ and $\xi^{cl}(\theta)$, we obtained exactly same results by centered TVD schemes for both choice of smoothness measure (r or s) .

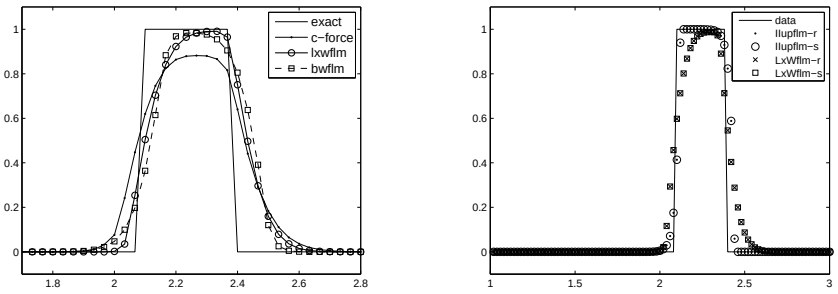

(a) (b)

FIG. 5.6. *Numerical result at* $T = 2.0$ *obtained by flux limited schemes using limiter (a)* $\xi^{cl}(r)$*,* $a\lambda = 0.8$ *and* $N = 90$*, (b)* $\xi^2(\theta)$*,* $a\lambda = 0.45$ *and* $N = 150$*.*

5.2.3. Buckley Leverett equation. A more demanding nonlinear scalar test equation is the Buckley-Leverett equation which models the two phase flows. It mimic the oil-recovery proccess and physically represents a mixture of oil and water through the porous medium. The scalar 1D equation is given by

$$\frac{\partial u}{\partial t} + \frac{\partial}{\partial x}\left(\frac{u^2}{u^2 + \frac{1}{4}(1-u)^2}\right) = 0 \tag{5.9}$$

Consider (5.9) alongwith following initial condition

$$u(x,0) = \begin{cases} 1, & \text{if } -\frac{1}{2} \le x \le 0, \\ 0, & else. \end{cases} \tag{5.10}$$

The solution involves two right moving shocks, each followed by an rarefaction wave. Numerical result obtained by hybrid scheme with compressive limiters is shown in Figure 5.7.

6. Conclusion and future work. In this work, flux limiter based high resolution schemes are investigated and classified based on two distinct TV stability regions. It is shown that both class of schemes give crisp resolution for discontinuities in opposite way. Universal TV stability region is proposed along with limiters which are some what diffusive but are robust as

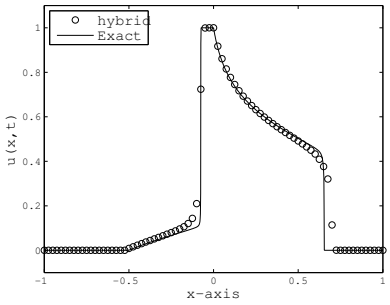

FIG. 5.7. *Buckley Leverett equation: Numerical result using compressive limiters* $\xi^{cl}(r)$ *for* $\lambda \max_u |f^{'}(u)| = 0.6,\ N = 80,\ T = 0.4$

they work for both class of schemes and give better accuracy compared to classical minmod limiter. By using the approach presented and other new results, construction of hybrid TVD flux limited schemes which can give atleast second order of accuracy even at extreme points is under progress.

Acknowledgments. The author would like to thank the referees for their helpful suggestions.

REFERENCES

[1] M. ARORA AND P. L. ROE, *A well-behaved tvd limiter for high-resolution calculations of unsteady flow*, Journal of Computational Physics, 132 (1997), pp. 3 – 11.

[2] S. F. DAVIS, *A simplified tvd finite difference scheme via artificial viscosity*, SIAM J. Sci. and Stat. Comput., 8 (1987), pp. pp. 1–18.

[3] A. HARTEN, *High resolution schemes for hyperbolic conservation laws,*, Journal of Computational Physics, 49 (1983), pp. 357 – 393.

[4] A. HARTEN, B. ENGQUIST, S. OSHER, AND S. R. CHAKRAVARTHY, *Uniformly high order accurate essentially non-oscillatory schemes, iii*, Journal of Computational Physics, 71 (1987), pp. 231 – 303.

[5] H. HASSANZADEH, J. ABEDI, AND M. POOLADI-DARVISH, *A comparative study of flux-limiting methods for numerical simulation of gas-solid reactions with arrhenius type reaction kinetics*, Computers & Chemical Engineering, 33 (2009), pp. 133 – 143.

[6] M. KADALBAJOO AND R. KUMAR, *A high resolution total variation diminishing scheme for hyperbolic conservation law and related problems*, Applied Mathematics and Computation, 175 (2006), pp. 1556 – 1573.

[7] M. J. KERMANI, A. G. GERBER, AND J. M. STOCKIE, *Thermodynamically based moisture prediction using roe's scheme*, Fourth conference of Iranian Aerospace Society Amir Kabir University of Technology, Tehran, Iran, (2003), pp. 27–29.

[8] B. KOREN, *A robust upwind discretization method for advection, diffusion and source terms*, Numerical methods for advection-diffusion problems, (1993), p. 117.

[9] R. KUMAR AND M. KADALBAJOO, *A class of high resolution shock capturing schemes for hyperbolic conservation laws*, Applied Mathematics and Computation, 195 (2008), pp. 110 – 126.

[10] C. B. LANEY, *Computational gasdynamics*, Cambridge University Press, 1998.

[11] R. J. LEVEQUE, *Numerical Methods for Conservation Laws*, Lectures in mathematics ETH Zürich, Birkhäuser Basel, 2nd ed., Feb. 1992.

[12] F. S. LIEN AND M. A. LESCHZINER, *Upstream monotonic interpolation for scalar transport with application to complex turbulent flows*, International Journal for Numerical Methods in Fluids, 19 (1994), pp. 527–548.

[13] S. PIPERNO AND S. DEPEYRE, *Criteria for the design of limiters yielding efficient high resolution tvd schemes*, Computers & Fluids, 27 (1998), pp. 183 – 197.

[14] W. J. RIDER, *A comparison of tvd lax-wendroff methods*, Communications in Numerical Methods in Engineering, 9 (1993), pp. 147–155.

[15] P. L. ROE, *Some contributions to the modeling of discontinuous flow*, Lectures in Applied Mathematics, 22 (1985), pp. 163–192.

[16] ———, *Characteristic-based schemes for the euler equations*, Annual Review of Fluid Mechanics, 18 (1986), pp. 337–365.

[17] C. W. SHU AND S. OSHER, *Efficient implementation of essentially non-oscillatory shock-capturing schemes*, J. Comput. Phys., 77 (1988), pp. 439–471.

[18] G. A. SOD, *A survey of several finite difference methods for systems of nonlinear hyperbolic conservation laws*, Journal of Computers, (1978), pp. 1–31.

[19] P. K. SWEBY, *High resolution schemes using flux limiters for hyperbolic conservation laws*, Siam Journal on Numerical Analysis, 21 (1984), pp. 995–1011.

[20] E. F. TORO, *Riemann Solvers and Numerical Methods for Fluid Dynamics: A Practical Introduction*, Springer, 3rd ed., Apr. 2009.

[21] E. F. TORO AND S. J. BILLETT, *Centred tvd schemes for hyperbolic conservation laws*, IMA Journal of Numerical Analysis, 20 (2000), pp. 47–79.

[22] B. VAN LEER, *Towards the ultimate conservative difference scheme. ii. monotonicity and conservation combined in a second-order scheme*, Journal of Computational Physics, 14 (1974), pp. 361 – 370.

[23] N. WATERSON AND H. DECONINCK, *Design principles for bounded higher-order convection schemes a unified approach*, Journal of Computational Physics, 224 (2007), pp. 182 – 207.

[24] H. YANG, *On wavewise entropy inequalities for high-resolution schemes. i: the semidiscrete case*, Math. Comp., 65 (1996), p. 4567.

[25] H. C. YEE, *Construction of explicit and implicit symmetric tvd schemes and their applications*, Journal of Computational Physics, 68 (1987), pp. 151 – 179.

[26] H. C. YEE, *Upwind and Symmetric Shock-Capturing Schemes*, tech. report, NASA Ames Research Center, May 1987.